University of HUDDERSFIELD

University of Huddersfield Repository

Kershaw Cook, Laurence J., Fisher, Julie, Harding, Lindsay P. and Halcrow, Malcolm A.

An iron(ii) spin-crossover metallacycle from a back-to-back bis-[dipyrazolylpyridine]

Original Citation

This version is available at http://eprints.hud.ac.uk/26923/

http://eprints.hud.ac.uk/

An iron(II) spin-crossover metallacycle from a back-to-back bis-[dipyrazolylpyridine]†

Laurence J. Kershaw Cook,[a] Julie Fisher,[a] Lindsay P. Harding[b] and Malcolm A. Halcrow*[a]

The syntheses of 4-mercapto-2,6-di(pyrazol-1-yl)pyridine (bppSH) and bis[2,6-di(pyrazol-1-yl)pyrid-4-yl]disulfide (bppSSbpp) are reported. In contrast to previously published "back-to-back" bis-[2,6-di(pyrazol-1-yl)pyridine] derivatives, which form coordination polymers with transition ions that are usually insoluble, bppSSbpp yields soluble oligomeric complexes with iron(II) and zinc(II). Mass spectrometry and DOSY data show that $[\{Fe(\mu\text{-}bppSSbpp)\}_n]^{2n+}$ and $[\{Zn(\mu\text{-}bppSSbpp)\}_n]^{2n+}$ form tetranuclear metallacycles in nitromethane solution ($n = 4$), although ^{1}H NMR and conductivity measurements imply the iron compound may undergo more fragmentation than its zinc congener. Both $[\{Fe(bppSH)_2\}]^{2+}$ and $[\{Fe(\mu\text{-}bppSSbpp)\}_n]^{2n+}$ exhibit thermal spin-crossover in CD_3NO_2 solution, with midpoint temperatures near 245 K. The similarity of these equilibria implies there is little cooperativity between the iron centres in the metallacyclic structures.

Introduction

One of the most useful series of compounds in the field of spin-crossover research[1–5] has proven to be $[Fe(bpp)_2]^{2+}$, where bpp is 2,6-di(pyrazol-1-yl)pyridine or a derivative of it (Scheme 1).[6–8] Two particular properties of $[Fe(bpp)_2]^{2+}$ centres account for their ubiquity. First, is that procedures are available to functionalise every position of the bpp ligand skeleton with a range of substituents.[1,3] Second, is that they often exhibit spin-state transitions at or near room temperature.[1,2] Thus, this has afforded molecular switches based on $[Fe(bpp)_2]^{2+}$ spin-transition centres bearing peripheral fluorescent,[9] conducting[10] or photo-isomerisable substituents,[11] yielding complexes combining spin-crossover with those functionalities. Alternatively, $[Fe(bpp)_2]^{2+}$ complexes with appropriate tether substituents have been used to form switchable surface nanostructures[12–14] and single-molecule junctions.[15] $[Fe(bpp)_2]^{2+}$ derivatives bearing protic or basic pyridyl substituents have proven useful in studies of the crystal engineering of supramolecular switching assemblies.[13,16,17] Finally, 'back-to-back' ligands with two bpp metal-binding domains linked
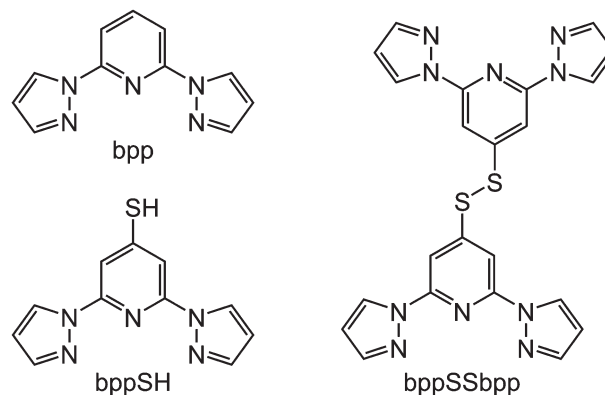
Scheme 1 The ligands discussed in this work.

through their pyridyl groups, have yielded 1D coordination polymers with spin-crossover functionality.[14,18,19]

A group of compounds from the bpp family that have not been investigated until now are derivatives bearing sulfur substituents at their pyridyl ring, of which 4-mercapto-2,6-di(pyrazol-1-yl)pyridine (bppSH) is the parent (Scheme 1). While such compounds could be used in self-assembled monolayers‡, bppSH is also of interest as a precursor to larger assembly structures through disulfide formation, or alkylation or ligation of the peripheral thiyl group. Such assemblies have

[a]*School of Chemistry, University of Leeds, Woodhouse Lane, Leeds, UK LS2 9JT.*
E-mail: m.a.halcrow@leeds.ac.uk; Fax: +44 (0)113 343 6565;
Tel: +44 (0)113 343 6506
[b]*Department of Chemical and Biological Sciences, University of Huddersfield, Huddersfield, UK HD1 3DH*

‡The chemistry of bppSH and its iron complexes on a gold surface will be described in a future publication.
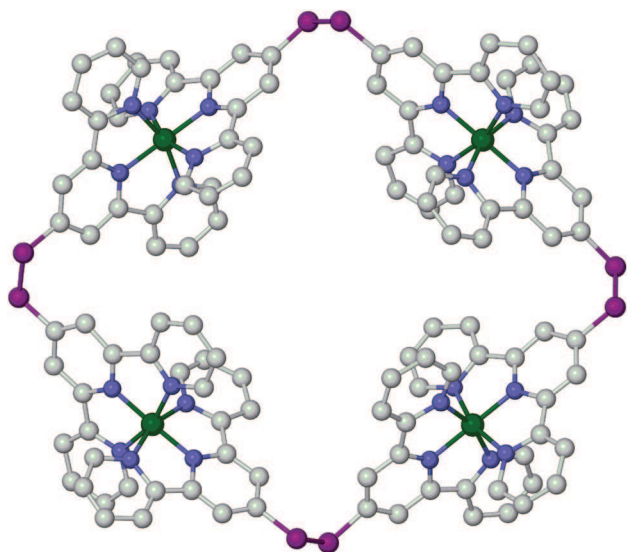
Fig. 1 Crystallographic structure of the [{Fe(μ-terpySSterpy)}₄]⁸⁺ metalla-cycle (data taken from ref. 20). The [{M(μ-bppSSbpp)}₄]⁸⁺ (M = Fe or Zn) assemblies in this work are proposed to have the same connectivity as this structure. Colour code: C, white; Fe, green; N, blue; S, pink.

been produced using closely related [Fe(terpySH)₂]²⁺ as a component (terpySH = 4′-mercapto-2,2′:6′,2″-terpyridine).[20–23] For example, the disulfide bis[2,2′:6′,2″-terpyridine-4′-yl]-disulfide (terpySSterpy) produces a cyclic oligomer [{Fe-(μ-terpySSterpy)}₄]⁸⁺ when complexed to iron(II), which was crystallographically characterised (Fig. 1).[20,24] We reasoned that a comparable metallacycle based on bis[2,6-di(pyrazol-1-yl)pyrid-4-yl]disulfide (bppSSbpp) could be a new type of multimetallic spin-crossover assembly.[25–28] We therefore now report the synthesis of bppSH and bppSSbpp, and a study of their coordination chemistry.

Results and discussion

Following a literature method for terpySH,[20] reaction of 4-iodo-2,6-di(pyrazolyl)pyridine[16] with NaSH in refluxing dmf affords bppSH in almost quantitative yield. Interestingly, its character-isation data imply that bppSH exists as its thiol tautomer (form A, Scheme 2), rather than as the alternative thione tauto-mer adopted by 4-mercaptopyridine (form B).[29] The evidence includes a strong ν(S–H) vibration at 2526 cm⁻¹, and the absence of a comparable ν(N–H) stretch, in the solid state IR spectrum of bppSH; and, the appearance of its pyridyl C^4 NMR resonance at 152.1 ppm in CDCl₃, essentially identical to that shown by the disulfide bppSSbpp described below (a thione tautomer would exhibit this peak near 195 ppm[29]). In contrast, terpySH exists as the thione tautomer in the single crystal,[20] but has been reported to be either pure thione or a mixture of both forms in solution.[20,21] The preference of bppSH for the thiol form may reflect the electron withdrawing nature of its pyrazolyl substituents, which could make its central pyridyl
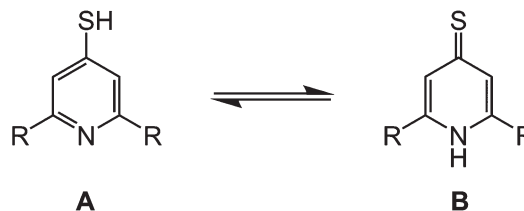
Scheme 2 The tautomeric equilibrium exhibited by 4-mercaptopyri-dines, between thiol (**A**) and thione (**B**) forms. bppSH (R = pyrazolyl) exhibits form A, but terpySH (R = pyridyl) predominantly adopts form B.

group insufficiently basic to deprotonate the thiol group (p$K_a \approx 5^{30}$).

Solutions of bppSH in air oxidise slowly to bis[2,6-di(pyrazol-1-yl)pyrid-4-yl]disulfide (bppSSbpp) over a period of days. The same reaction was achieved almost quantitatively by oxidation of bppSH with I₂ in the presence of base. The iden-tity of bppSSbpp was confirmed by mass spectrometry (m/z = 507.1, corresponding to [Na(bppSSbpp)]⁺) and by a crystal structure determination (Fig. 2). The coplanar, transoid dis-position of the heterocyclic rings in each dipyrazolylpyridyl (bpp) fragment is typical for this class of compound.[31] The torsion angle about the disulfide group is 82.45(7)° and the two bpp metal-binding domains in the molecule are almost perfectly perpendicular to each other, the dihedral angle between them being 88.86(2)°. The molecules in the crystal associate into 1D stacks *via* π···π interactions between bpp fragment N(19)–C(36) and its symmetry equivalents N(19^i)–C(36^i) and N(19^{ii})–C(36^{ii}) (symmetry codes (ii) −x, 2 − y, −z; (ii) 1 − x, 2 − y, −z), which are related by crystallographic inversion centres translating along a. These stacks are in turn linked by another pairwise π···π interaction, between bpp the moieties N(1)–C(16) and N(1^{iii})–C(16^{iii}) (symmetry code (iii) 1 − x, 2 − y, 1 − z). In each case the interacting bpp fragments are coplanar by symmetry, and separated by 3.508(4)–3.510(4) Å (ESI†).

Two salts [Fe(bppSH)₂]X₂ (X⁻ = BF₄⁻, **1[BF₄]₂**; X⁻ = BF₄⁻, **1[ClO₄]₂**) were prepared by treatment of the appropriate metal
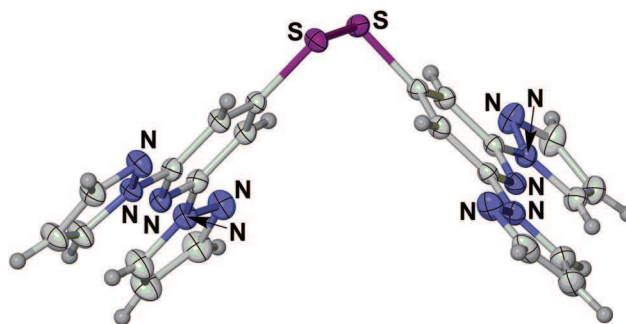

Fig. 2 View of the unique molecule in the crystal structure of bppSSbpp, emphasising the right-angled disposition of the metal-binding bpp moieties. Atomic displacement ellipsoids are drawn at the 50% probability level. Colour code: C, white; H, grey; N, blue; S, pink.

salt with 2 equiv. bppSH. Both salts precipitate from organic solvents as mixtures of polycrystalline and amorphous material by X-ray powder diffraction, which contain lattice water according to microanalysis (ESI†). Neither salt was obtained in single crystal form. Magnetic susceptibility measurements showed that both salts exhibit temperature-dependent spin-state behaviour in the solid state. However, only $1[ClO_4]_2$ exhibits a well-defined spin-transition, which involves *ca.* 60% of the sample and is superimposed on a much more gradual spin-equilibrium involving the remainder of the material. The transition occurs with midpoint temperature $T_{1/2} = 240$ K and, unusually, exhibits a 15 K thermal hysteresis loop (ESI†). The first derivative of the $\chi_M T$ *vs. T* curve implies that both sides of the hysteretic transition are split into two components separated by 3–4 K, which was confirmed by a DSC measurement. Since $1[ClO_4]_2$ has the greatest degree of crystallinity of the two salts, its hysteretic spin-transition can be attributed to the crystalline fraction of the material. However, the structural origin of this unusually cooperative transition could not be investigated further in the absence of a single crystal structure.

Treatment of hydrated $Fe[BF_4]_2$ or $Fe[ClO_4]_2$ with 1 equiv. bppSSbpp in nitromethane yields homogeneous solutions, whose orange colour is characteristic of $[Fe(bpp)_2]^{2+}$-type centres. Attempted crystallisation of the products from these solutions by slow solvent diffusion methods yielded intractable oils, and the complexes could only be isolated as solids by evaporation of the solutions to dryness. The solid residues were washed with diethyl ether, dried *in vacuo* and analysed without further purification. This yielded $[\{Fe(\mu\text{-}bppSSbpp)\}_n]$-$X_{2n}$ ($X^- = BF_4^-$, $2[BF_4]_2$; $X^- = ClO_4^-$, $2[ClO_4]_2$). Since the iron compounds are paramagnetic (see below), the diamagnetic zinc(II) analogue $[\{Zn(\mu\text{-}bppSSbpp)\}_n][BF_4]_{2n}$ ($3[BF_4]_2$) was also prepared by the same method, for the purposes of NMR characterisation. All three of these compounds retained 1/4–1/2 equiv. of diethyl ether per metal ion in the solid state by microanalysis, which was also visible in their ^{1}H NMR spectra. The solubility of $2[BF_4]_2$, $2[ClO_4]_2$ and $3[BF_4]_2$ in organic solvents is striking, since other back-to-back bis-bpp ligands without solubilising substituents afford insoluble coordination polymers when complexed to iron(II).[18,19]

These materials are completely amorphous powders by X-ray powder diffraction (ESI†). At 298 K, solid $2[BF_4]_2$ and $2[ClO_4]_2$ both exhibit $\chi_M T$ (per Fe atom) = 2.9 cm^3 mol^{-1} K, showing they are predominantly high-spin at room temperature; a small low-spin population at room temperature is consistent with their red-orange colouration. Both samples undergo gradual and incomplete thermal spin-crossover equilibria, which are almost monotonic between 100–350 K but exhibit a 40–50% residual high-spin fraction frozen in below that temperature (Fig. 3). Such gradual and poorly defined spin-crossover is typical for amorphous samples, with a distribution of molecular environments in a heterogeneous solid matrix.

The room temperature ^{1}H NMR spectrum of $3[BF_4]_2$ in the weakly interacting solvent CD_3NO_2 is broadened, but contains
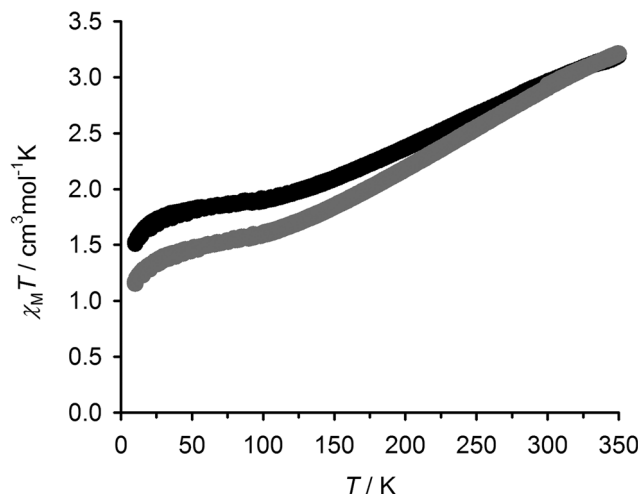

Fig. 3 Variable temperature magnetic susceptibility data for solid $2[BF_4]_2$ (●) and $2[ClO_4]_2$ (◉). The $\chi_M T$ data are quoted per mole equivalent of Fe.

peaks attributable to one metal-bound bpp domain, and a second minor component that may be an uncoordinated bpp fragment based on its chemical shifts. The integral ratio of coordinated : uncoordinated bpp residues in the spectrum is *ca.* 9 : 1. In contrast, the ^{1}H NMR spectra of paramagnetic $2[BF_4]_2$ and $2[ClO_4]_2$ contain contact-shifted peaks attributable to two metal-bound bpp environments with comparable intensities, and one uncoordinated bpp environment in the diamagnetic region. The ratio of coordinated : uncoordinated bpp residues cannot be quantified in these spectra, because the integrals of diamagnetic and contact-shifted NMR peaks are not directly comparable.[32] None-the-less, the spectra confirm that $2[BF_4]_2$ and $2[ClO_4]_2$ are high-spin at room temperature in solution, as well as in the solid state. The observation of different numbers of coordinated bpp environments for $2X_2$ ($X^- = BF_4^-$ and ClO_4^-) and $3[BF_4]_2$ was unexpected, and could have two explanations. The distribution of assembly structures in all the spectra could be similar, but in more rapid chemical exchange in $3[BF_4]_2$ than in $2X_2$. That seems unlikely, since zinc(II) and high-spin iron(II) exhibit comparable rates of ligand exchange in solution.[33] Alternatively, the CD_3NO_2 solutions of $2X_2$ and $3[BF_4]_2$ may contain different molecular assemblies.

These data were supported by variable temperature conductivity measurements in $MeNO_2$. A plot of $(\Lambda_0 - \Lambda_e)$ *vs.* $c^{1/2}$ (Λ_0 = conductivity at infinite dilution, Λ_e = measured conductivity and c = concentration) should yield a straight line whose slope is characteristic of the electrolyte composition of the solution.[34] Since such linear behaviour was exhibited by all the compounds, the speciation of the $[\{M(\mu\text{-}bppSSbpp)\}_n]^{2n+}$ (M = Fe and Zn) metallacycles does not change across the measured concentration range (Fig. 4).[35] The slope of the plot for $1[ClO_4]_2$ is 509, which is within the range expected for a 2 : 1 metal complex electrolyte in $MeNO_2$.[36] The slopes for $2[BF_4]_2$ (1312) and $2[ClO_4]_2$ and (1347) are identical within experimental error, implying that their anions do not
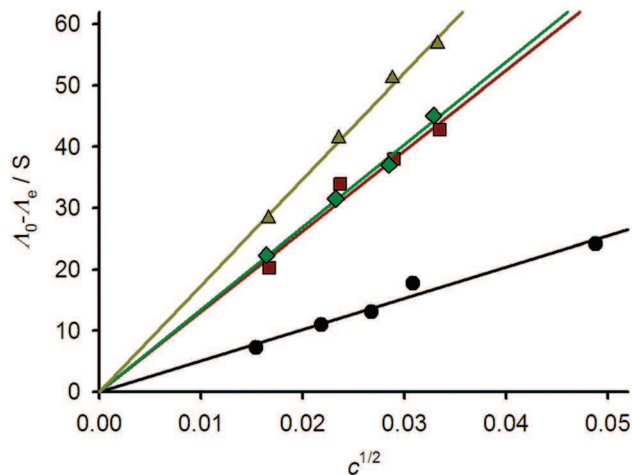
Fig. 4 Variable concentration conductivity plots for **1[ClO$_4$]$_2$** (black circles), **2[BF$_4$]$_2$** (red squares), **2[ClO$_4$]$_2$** (green diamonds) and **3[BF$_4$]$_2$** (yellow triangles).
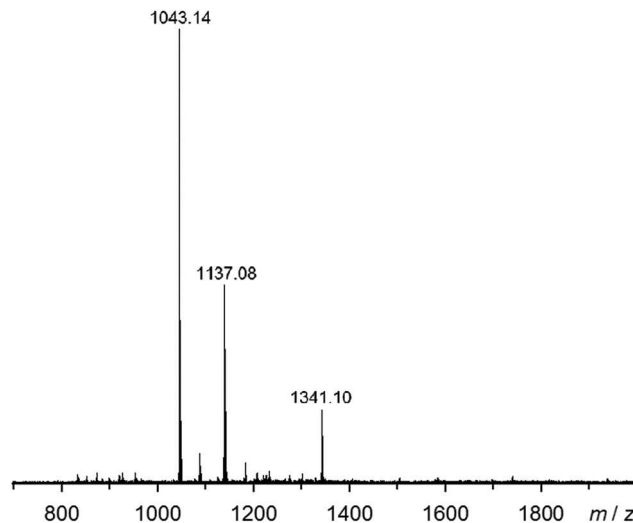
Fig. 5 Electrospray mass spectrum of **2[BF$_4$]$_2$** from MeNO$_2$ solution. The highlighted ions are [Fe(bppSSbpp)$_2$F]$^+$ (m/z = 1043.1); [Fe$_2$(bppSSbpp)$_2$(F)$_3$]$^+$ (m/z = 1137.1) and [Fe$_4$(bppSSbpp)$_4$(BF$_4$)$_6$]$^{2+}$ (m/z = 1341.1). The F$^-$ ions arise from metal-promoted hydrolysis of BF$_4^-$ under the conditions of the experiment. Other mass spectra and peak assignments are in the ESI.†

contribute to their aggregation structures.[37] Unexpectedly, however, a higher slope was obtained for **3[BF$_4$]$_2$** (1738). All these values are greater than expected for a 3 : 1 electrolyte in this solvent,[36] although the electrolyte type for these compounds cannot be determined more accurately because of the lack of appropriate reference data.[34]

The solution structure of **3[BF$_4$]$_2$** in CD$_3$NO$_2$ at 293 K was probed further by a diffusion oriented spectroscopy (DOSY) experiment,[38] which has been shown previously to be useful for metallacyclic assemblies.[39–41] The diffusion coefficient for the free bppSSbpp ligand under these conditions was 7.69 ± 0.56 × 10^{-10} m^2 s^{-1}. The DOSY analysis of **3[BF$_4$]$_2$** yielded just one aggregated species, with a diffusion coefficient of 3.58 ± 0.14 × 10^{-10} m^2 s^{-1} (ESI†). A smaller fraction of free bppSSbpp was also detected, supporting the presence of trace free ligand in the complex's ^{1}H NMR spectrum (see above). The ratio of the two diffusion coefficients is 0.46, which is lower than might be expected for a dimeric [{Zn(μ-bppSSbpp)}$_n$]$^{2n+}$ assembly (n = 2; theoretical monomer : dimer ratio ≈ 0.75) or an equilateral trimer (n = 3; monomer : trimer ratio ≈ 0.6),[42] but is significantly higher than has been measured for a cylindrical 16-mer assembly.[43]

Assuming a stick solvent/solute relationship,[44] the isotropic hydrodynamic radius of the [{M(μ-bppSSbpp)}$_n$]$^{2n+}$ assembly in **3[BF$_4$]$_2$** is 9.66 Å. That agrees excellently with the DOSY hydrodynamic radii for another series of tetranuclear metallacycles containing [M(terpy)$_2$]$^{2+}$ centres (r_H = 9.7 Å).[39] In contrast, larger hydrodynamic radii have been measured for hexameric (r_H = 11.3 Å) and nonameric (r_H = 11.8 Å) macrocycles of [M(terpy)$_2$]$^{2+}$ units.[41] The crystallographic dimensions of the [{Fe(μ-terpySSterpy)}$_4$]$^{8+}$ tetramer are *ca.* 11 × 25.5 × 25.5 Å,[20] yielding an averaged diameter of 20.7 Å, or radius of 10.3 Å. That is in reasonable agreement with the r_H value for **3[BF$_4$]$_2$**, particularly since the bpp metal-binding residues in bppSSbpp are slightly smaller than the terpy moieties in the literature compound.

Electrospray mass spectra of **2[BF$_4$]$_2$**, **2[ClO$_4$]$_2$** and **3[BF$_4$]$_2$** all show strong molecular ions, corresponding to the same three species: [M(bppSSbpp)$_2$X]$^+$, [M$_2$(bppSSbpp)$_2$X$_3$]$^+$ and [M$_4$(bppSSbpp)$_4$X$_6$]$^{2+}$ (M = Fe or Zn, X$^-$ = anion; Fig. 5 and ESI†). Each spectrum also contains a number of weaker ions with relative intensities 3–10%, most of which can be derived from the cyclic tetramer species by loss or gain of bppSSbpp, loss or gain of metal cations and anions, or fragmentation. Only **2[ClO$_4$]$_2$** shows clear evidence of other cyclic oligomers through weak ions assignable to [Fe$_3$(bppSSbpp)$_3$(ClO$_4$)$_4$]$^{2+}$ and [Fe$_5$(bppSSbpp)$_5$(ClO$_4$)$_8$]$^{2+}$, each of 2–3% relative abundance (ESI†). Hence, the mass spectrometry data also imply that tetrameric [{M(μ-bppSSbpp)}$_4$]$^{8+}$ (M = Fe or Zn) is the predominant oligomeric species in solutions of these compounds.

Variable temperature Evans method magnetic susceptibility measurements in CD$_3$NO$_2$ solution from **1[BF$_4$]$_2$** and **2[BF$_4$]$_2$** gave very similar results. Both complexes are almost completely high-spin at room temperature under these conditions, but exhibit the onset of a thermal spin equilibrium on cooling (Fig. 6). The midpoint temperatures of the equilibria ($T_{1/2}$) are both near the freezing point of the solvent, and can be estimated at 246 ± 1 K for **1[BF$_4$]$_2$** and 243 ± 1 K for **2[BF$_4$]$_2$**. These values are almost identical to the parent complex [Fe(bpp)$_2$]$^{2+}$ (Scheme 1), which exhibits $T_{1/2}$ = 248 K in (CD$_3$)$_2$CO[45] (the use of a different organic solvent will have a minimal effect on these data[46]). The thermodynamic parameters for the equilibria are likewise similar, with **1[BF$_4$]$_2$** exhibiting ΔH = 29(2) kJ mol^{-1} and ΔS = 120(8) J mol^{-1} K^{-1}; and for **2[BF$_4$]$_2$**, ΔH = 25(2) kJ mol^{-1} and ΔS = 104(8) J mol^{-1} K^{-1} (per mole of Fe). The larger-than-normal errors on those values arise because the equilibria could not be fully measured within the liquid range
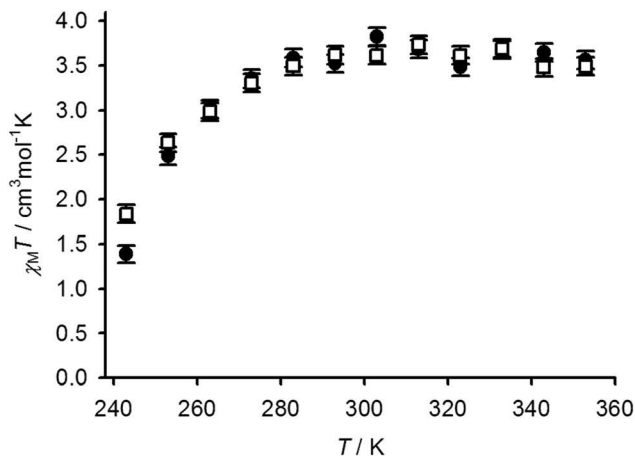
Fig. 6 Variable temperature magnetic susceptibility data in CD_3NO_2 solution for **1[BF$_4$]$_2$** (●) and **2[BF$_4$]$_2$** (□).

of the CD_3NO_2 solvent; use of a solvent with a lower freezing point in this work was precluded on solubility grounds. The slightly higher ΔH value for **1[BF$_4$]$_2$** might be evidence for ligand dissociation in the high-spin state of that compound, which could be promoted by the nucleophilic thiol substituents. Be that as it may, such a rapid pre-equilibrium would have no effect on the spin-crossover $T_{1/2}$.[47] Conversely, the ΔH value for **2[BF$_4$]$_2$** is at the high end of the usual range for [Fe(bpp)$_2$]$^{2+}$ derivatives in inorganic solvents.[45,46,48] That implies ligand displacement reactions play, at most, a minor role in the solution chemistry of **2[BF$_4$]$_2$**.[47] Hence, incorporation of the isolated [Fe(bpp)$_2$]$^{2+}$ centres in **1[BF$_4$]$_2$** into a metallacyclic structure in **2[BF$_4$]$_2$** has little effect on their spin state properties.

Conclusions

The new thiolated ligand 4-mercapto-2,6-di(pyrazol-1-yl)pyridine (bppSH) has been synthesised,‡ and converted to the dinucleating disulfide ligand bppSSbpp (Scheme 1). While iron(II) or zinc(II) complexes of other back-to-back bis-[dipyrazolylpyridine] derivatives have been made before, bppSSbpp is unique in forming soluble oligomer assemblies upon complexation with metal ions, rather than insoluble 1D coordination polymers. Mass spectrometry and DOSY data are both consistent with tetrameric metallacycles [{M(μ-bppSSbpp)}$_4$]$^{8+}$ (M = Fe or Zn) being the predominant species in solutions of these compounds. However, the conductivity data (Fig. 4) and ^1H NMR (ESI†) imply that the [{M(μ-bppSSbpp)}$_4$]$^{8+}$ assembly may undergo a greater degree of fragmentation or ring-opening when M = Fe than when M = Zn, under the conditions in this work. Since high-spin Fe^{2+} and Zn^{2+} are both labile metal ions that is an unexpected observation, but it might reflect the pronounced Jahn–Teller distortion that is often exhibited by high-spin [Fe(bpp)$_2$]$^{2+}$ centres.[6] The symmetry of the metallacycle would be disrupted if a fraction of the iron

centres in **2[BF$_4$]$_2$** and **2[ClO$_4$]$_2$** adopt this distorted geometry at room temperature, potentially leading to this increased fragmentation as observed. That would not be a factor for the zinc centres in **3[BF$_4$]$_2$** or the low-spin iron sites in [{Fe(μ-terpySSterpy)}$_4$]$^{8+}$ (Fig. 1), which are not Jahn–Teller active.

This study compliments Constable et al.'s earlier report of [{Fe(μ-terpySSterpy)}$_4$]$^{8+}$. That was characterised as a tetrameric metallacycle on the basis of a crystal structure (Fig. 1), but no solution phase data were reported. While we have been unable to crystallise **2[BF$_4$]$_2$**, **2[ClO$_4$]$_2$** or **3[BF$_4$]$_2$**, they form cyclic tetranuclear assemblies with minimal evidence for higher or lower cyclic oligomers, in the weakly associating solvent $MeNO_2$.[20] The apparent preference of these back-to-back bis-tridentate disulfides to form soluble, square metallacyclic complexes reflects the acute R–S–S–R torsions favoured by the disulfido group, which place the metal-binding domains approximately at right angles to each other (Fig. 2).[20] This contrasts with the *transoid* R–CH$_2$–CH$_2$–R torsion adopted by 1,2-bis[2,6-di(pyrazol-1-yl)pyrid-4-yl]ethane (bppC$_2$H$_4$bpp), for example, which instead forms insoluble coordination polymers upon reaction with iron(II) salts.[18]

Solid **2[BF$_4$]$_2$** and **2[ClO$_4$]$_2$** exhibit thermal spin-crossover, as predicted at the outset of this work, making this a new type of supramolecular spin-crossover assembly.[25–28] However, their spin-crossover transitions are gradual and incomplete at low temperatures, reflecting their amorphous nature in the solid state. In solution, **2[BF$_4$]$_2$** undergoes a thermal spin-state equilibrium at an almost identical temperature to the mononuclear precursor **1[BF$_4$]$_2$**, implying that the four iron centres in [{Fe(μ-bppSSbpp)}$_4$]$^{8+}$ undergo spin-crossover independently of each other under these conditions.

Experimental

Unless otherwise stated, all reactions were carried out in air using non-pre-dried AR-grade solvents. 4-Iodo-2,6-di(pyrazol-1-yl)pyridine was synthesised by the literature method,[16] while all other reagents were used as commercially supplied. Mass spectra for the metallacyclic complexes are tabulated and assigned in the ESI.†

Synthesis of 4-mercapto-2,6-di(pyrazol-1-yl)pyridine (bppSH)

Addition of NaSH·H$_2$O (2.70 g, 36.4 mmol) to 4-iodo-2,6-di(pyrazol-1-yl)pyridine (0.49 g, 1.45 mmol) in dimethylformamide (100 cm^3) caused a darkening of the solution to a deep green color. The solution was refluxed for 4 h, then cooled to room temperature. The solvent was removed *in vacuo* leaving a pale yellow residue which was taken up in water (50 cm^3) and neutralised with concentrated HCl which precipitated a cream-coloured solid. This was collected by filtration and dried *in vacuo*. Yield 0.35 g, 96%. Found: C 54.4, H 3.55, N 28.5%. Calcd for C$_{11}$H$_9$N$_5$S C 54.3, H 3.73, N 28.8%. M.p. 133–135 °C. ES mass spectrum: m/z 266.0 [Na(bppSH)]$^+$. ^1H NMR (300 MHz, {CD$_3$}$_2$SO); δ, ppm 6.60 (dd, J = 1.7 and 2.5 Hz, 2H, pz H^4), 7.82 (s, 2H, py $H^{3/5}$), 7.84 (d, 1.7 Hz, 2H, pz H^3),

8.87 (d, 2.5 Hz, 2H, pz H^5). ^{13}C NMR (75.5 MHz, {CD$_3$}$_2$SO); δ, ppm 106.6 (2C, py $C^{3/5}$), 108.5 (2C, pz C^4), 128.2 (2C, pz C^5), 142.7 (2C, pz C^3), 149.5 (2C, pz $C^{2/6}$), 152.1 (1C, py C^4).

Synthesis of bis(2,6-di[pyrazol-1-yl]pyridin-4-yl)disulfide (bppSSbpp)

NaOH (29 mg, 0.0.73 mmol) and I$_2$ (84 mg, 0.33 mmol) were added to a stirring suspension of bppSH (0.15 g, 0.62 mmol) in H$_2$O (15 cm^3) at room temperature. Stirring was continued for 20 h, yielding a cream-coloured precipitate. The off-white solid was collected, washed with further H$_2$O, EtOH and Et$_2$O and dried over P$_2$O$_5$. Yield 0.14 g, 91%. Found C 54.3, H 3.25, N 29.1%. Calcd for C$_{22}$H$_{16}$N$_{10}$S$_2$ C 54.5, H 3.33, N 28.9%. M.p. 240–242 °C. ES mass spectrum: m/z 507.1 [Na(bppSSbpp)]$^+$. ^{1}H NMR (300 MHz, CDCl$_3$); δ, ppm 6.47 (t, 2.1 Hz, 4H, pz H^4), 7.74 (br s, 4H, pz H^3), 8.02 (s, 4H, py $H^{3/5}$), 8.51 (d, 2.1 Hz, 4H, pz H^5); ^{13}C NMR (75.5 MHz, CDCl$_3$); δ, ppm 105.4 and 108.2 (both 2C, py $C^{3/5}$ and pz C^4), 127.3 (2C, pz C^5), 142.7 (2C, pz C^3), 150.4 (2C, Py $C^{2/6}$), 152.4 (1C, Py C^4).

Synthesis of [Fe(bppSH)$_2$][BF$_4$]$_2$ (1[BF$_4$]$_2$)

A mixture of Fe[BF$_4$]$_2$·6H$_2$O (0.11 g, 0.32 mmol) and bppSH (0.17 g, 0.64 mmol) in MeNO$_2$ (40 cm^3) was stirred under N$_2$ for 2 h, until all the solid had dissolved. The opaque yellow-orange solution was filtered, and excess Et$_2$O (100 cm^3) was added to the filtrate, precipitating the yellow product which was collected and desiccated. Yield 0.18 g, 76%. Found: C, 35.1; H, 2.70; N, 18.6%. Calcd for C$_{22}$H$_{18}$B$_2$FeN$_{10}$F$_8$S$_2$·2H$_2$O: C, 35.1; H, 2.95; N, 18.6%. ^{1}H NMR (CD$_3$NO$_2$) δ 36.9 and 38.1 (both 4H, Py $H^{3/5}$ and Pz H^5), 55.4 (4H, Pz H^4), 64.8 (4H, Pz H^3).

Synthesis of [Fe(bppSH)$_2$][ClO$_4$]$_2$ (1[ClO$_4$]$_2$)

Method as for **1[BF$_4$]$_2$**, using Fe[ClO$_4$]$_2$·6H$_2$O (0.12 g, 0.32 mmol). Slow addition of degassed iPr$_2$O (25 cm^3) to the filtered solution caused the formation of a yellow solid. This was collected by filtration, washed with a further few drops of iPr$_2$O and dried *in vacuo*. Yield 0.18 g, 73%. Found: C, 35.1; H, 2.40; N, 18.2%. Calcd for C$_{22}$H$_{18}$Cl$_2$FeN$_{10}$O$_8$S$_2$·H$_2$O: C, 34.8; H, 2.65; N, 18.4%.

Synthesis of [Fe(bppSSbpp)][BF$_4$]$_2$ (2[BF$_4$]$_2$)

Solid Fe[BF$_4$]$_2$·6H$_2$O (49 mg, 0.15 mmol) was added to a suspension of bppSSbpp (70 mg, 0.14 mmol) in MeNO$_2$ (30 cm^3). The solution was stirred at room temperature for 30 min, and then filtered. The solvent was removed *in vacuo* to give a brick-red microcrystalline solid, which was washed with diethyl ether and dried *in vacuo*. Yield 77.0 mg, 77%. Found: C, 38.2; H, 3.05; N, 18.6%. Calcd for C$_{22}$H$_{16}$B$_2$F$_8$N$_{10}$S$_2$Fe·1/2Et$_2$O C, 38.4; H, 2.82; N, 18.6%. ^{1}H NMR (CD$_3$NO$_2$) species 1: δ 37.5 and 38.1 (both 4H, Py H^3 + Pz H^5), 56.4 (4H, Pz H^4), 65.7 (4H, Pz H^3); species 2: δ 37.3 and 38.7 (both 4H, Py H^3 + Pz H^5), 56.9 (4H, Pz H^4), 66.1 (4H, Pz H^3); species 3: δ 6.55 (br s, 2H, pz H^4), 7.69 and 7.80 (both br s, 2H, pz H^3 and py $H^{3/5}$), 8.66 (br s, 2H, pz H^5).

Synthesis of [Fe(bppSSbpp)][ClO$_4$]$_2$ (2[ClO$_4$]$_2$)

Method as for **1[BF$_4$]$_2$**, using Fe[ClO$_4$]$_2$·6H$_2$O (54 mg, 0.15 mmol). The product was an orange-brown solid. Yield 52 mg, 44%. Found: C, 36.1; H, 2.60; N, 18.2%. Calcd for C$_{22}$H$_{16}$Cl$_2$FeN$_{10}$O$_8$S$_2$·1/4Et$_2$O: C, 36.4; H, 2.72; N, 18.4%. ^{1}H NMR (CD$_3$NO$_2$) δ 37.4 and 38.1 (both 4H, Py H^3 + Pz H^5), 55.5 (4H, Pz H^4), 64.9 (4H, Pz H^3).

Synthesis of [Zn(bppSSbpp)][BF$_4$]$_2$ (3[BF$_4$]$_2$)

Solid Zn[BF$_4$]$_2$·6H$_2$O (51 mg, 0.15 mmol) and bppSSbpp (70 mg, 0.14 mmol) were stirred together in a 1 : 2 MeNO$_2$–MeCN solvent mixture (20 cm^3) for 1 h. The solvents were removed from the filtered solution and the pale yellow oily residue was triturated in Et$_2$O (80 cm^3), yielding a colourless polycrystalline solid that was collected by filtration. Yield 65.0 mg, 64%. Found: C, 38.1; H, 2.90; N, 18.5%. Calcd for C$_{22}$H$_{16}$B$_2$F$_8$N$_{10}$S$_2$Zn·1/2Et$_2$O: C, 37.9; H, 2.78; N, 18.4%. ^{1}H NMR (CD$_3$NO$_2$) major species: δ 6.67 (br s, 4H, Pz H^4), 7.65 (br s, 4H, Pz H^3), 8.18 (br s, 4H, Py $H^{3/5}$), 8.68 (br s, 4H, Pz H^5): minor species: δ 6.38, 7.58, 7.77; ^{13}C NMR (CD$_3$NO$_2$) major species: δ 106.9 (Py $C^{3/5}$), 113.1 (Pz C^4), 131.5 (Pz C^5), 144.5 (Pz C^3), 147.0 (Py $C^{2/6}$), 155.6 (Py C^4).

Single crystal X-ray structure determination

Diffraction data were measured using a Bruker X8 Apex II diffractometer, with graphite-monochromated Mo-K$_\alpha$ radiation (λ = 0.71073 Å) generated by a rotating anode. The diffractometer was fitted with Oxford Cryostream low-temperature device. Experimental details of the structure determination are given in Table 1. The structure was solved by direct methods (*SHELXS97*[49]), and developed by full least-squares refinement on F^2 (*SHELXL97*[49]). Crystallographic figures were prepared using *XSEED*,[50] which incorporates *POVRAY*.[51]

No disorder is present in the model, and no restraints were applied. All non-H atoms were refined anisotropically, and all H atoms were located in the Fourier map and allowed to refine freely. Refined C–H distances range from 0.93(2)–1.01(2) Å.

Table 1 Experimental details for the crystal structure determination of bppSSbpp

Molecular formula	C$_{22}$H$_{16}$N$_{10}$S$_2$	V (Å^3)	1144.5(3)
M_r	484.57	Z	2
Crystal class	Triclinic	μ (mm^{-1})	0.266
Space group	$P\bar{1}$	T (K)	150(2)
a (Å)	8.9223(13)	Measured reflections	36 263
b (Å)	10.2903(14)	Independent reflections	7730
c (Å)	13.341(2)	R_{int}	0.052
α (°)	90.512(6)	R_1, $I > 2\sigma(I)^a$	0.041
β (°)	107.862(7)	wR_2, all data^b	0.141
γ (°)	100.271(6)	Goodness of fit	1.148

^{a} $R = \sum[|F_o| - |F_c|]/\sum|F_o|$. ^{b} w$R = [\sum w(F_o^2 - F_c^2)/\sum w F_o^4]^{1/2}$.

Other measurements

Elemental microanalyses were performed by the University of Leeds School of Chemistry microanalytical service. Electrospray mass spectra were recorded from 10^{-3} M solutions on a Bruker MicroTOF-q instrument, from $CHCl_3$ solution (organic compounds) or CH_3NO_2 solution (metal complexes). X-ray powder diffraction patterns were measured using a Bruker D2 Phaser diffractometer.

Variable temperature magnetic susceptibility measurements were performed on a Quantum Design SQUID/VSM magnetometer, in an applied field of 5000 G. A diamagnetic correction for the sample was estimated from Pascal's constants;[52] a diamagnetic correction for the sample holder was also measured separately, and applied to the data. Magnetic susceptibility measurements in solution were obtained by Evans method using a Bruker DRX500 spectrometer operating at 500.13 MHz.[53] A diamagnetic correction for the sample,[52] and a correction for the variation of the density of the CD_3NO_2 solvent with temperature,[54] were applied to these data. All magnetochemical data manipulation was carried out using *SIGMAPLOT*.[55]

DOSY NMR measurements in CD_3NO_2 were obtained using a Varian Inova 500 MHz spectrometer, with a 5 mm ID probe. A bipolar pulse pair stimulated echo (*BBPSTE*) pulse sequence[56] was employed, operating in the *ONESHOT* experiment.[57] Additional parameters: number of different gradient levels, 15; gradient stabilization delay, 0.003 s; gradient length, 0.02–0.03 s; relaxation delay, 12 s; acquisition time, 1.3 s; number of data points, 8192 pairs; spectral width, 6000 Hz. Data were processed with a 1 Hz line broadening prior to Fourier transformation and baseline correction. The concentration of the sample was 0.8 mM.

Acknowledgements

Notes and references

1 *Spin Crossover in Transition Metal Compounds I-III*, ed. P. Gütlich and H. A. Goodwin, *Top. Curr. Chem.*, 2004, vol. 233–235.

2 *Spin-crossover materials - properties and applications*, ed. M. A. Halcrow, John Wiley & Sons, Chichester, 2013, p. 568.

3 A. Bousseksou, G. Molnár, L. Salmon and W. Nicolazzi, *Chem. Soc. Rev.*, 2011, **40**, 3313.

4 M. A. Halcrow, *Chem. Soc. Rev.*, 2011, **40**, 4119.

5 For other recent reviews see: M. C. Muñoz and J. A. Real, *Coord. Chem. Rev.*, 2011, **255**, 2068; J. Tao, R.-J. Wei, R.-B. Huang and L.-S. Zheng, *Chem. Soc. Rev.*, 2012, **41**,

703; P. Gütlich, *Eur. J. Inorg. Chem.*, 2013, 581; P. Gütlich, A. B. Gaspar and Y. Garcia, *Beilstein J. Org. Chem.*, 2013, **9**, 342; P. Guionneau, *Dalton Trans.*, 2014, **43**, 382.

6 M. A. Halcrow, *Coord. Chem. Rev.*, 2009, **253**, 2493; L. J. Kershaw Cook, R. Mohammed, G. Sherborne, T. D. Roberts, S. Alvarez and M. A. Halcrow, *Coord. Chem. Rev.*, 2015, **289–290**, 2.

7 J. Olguín and S. Brooker, *Coord. Chem. Rev.*, 2011, **255**, 203.

8 M. A. Halcrow, *New J. Chem.*, 2014, **38**, 1868.

9 R. González-Prieto, B. Fleury, F. Schramm, G. Zoppellaro, R. Chandrasekar, O. Fuhr, S. Lebedkin, M. Kappes and M. Ruben, *Dalton Trans.*, 2011, **40**, 7564.

10 M. Nihei, N. Takahashi, H. Nishikawa and H. Oshio, *Dalton Trans.*, 2011, **40**, 2154.

11 Y. Hasegawa, K. Takahashi, S. Kume and H. Nishihara, *Chem. Commun.*, 2011, **47**, 6846; K. Takahashi, Y. Hasegawa, R. Sakamoto, M. Nishikawa, S. Kume, E. Nishibori and H. Nishihara, *Inorg. Chem.*, 2012, **51**, 5188.

12 M. S. Alam, M. Stocker, K. Gieb, P. Müller, M. Haryono, K. Student and A. Grohmann, *Angew. Chem., Int. Ed.*, 2010, **49**, 1159.

13 M. Cavallini, I. Bergenti, S. Milita, J. C. Kengne, D. Gentili, G. Ruani, I. Salitros, V. Meded and M. Ruben, *Langmuir*, 2011, **27**, 4076.

14 K. Botcha, S. Basak and R. Chandrasekar, *RSC Adv.*, 2014, **4**, 34760.

15 D. Secker, S. Wagner, S. Ballmann, R. Härtle, M. Thoss and H. B. Weber, *Phys. Rev. Lett.*, 2011, **106**, 136807; V. Meded, A. Bagrets, K. Fink, R. Chandrasekar, M. Ruben, F. Evers, A. Bernand-Mantel, J. S. Seldenthuis, A. Beukman and H. S. J. van der Zant, *Phys. Rev. B: Condens. Matter*, 2011, **83**, 245415.

16 C. Rajadurai, F. Schramm, S. Brink, O. Fuhr, M. Ghafari, R. Kruk and M. Ruben, *Inorg. Chem.*, 2006, **45**, 10019.

17 I. Šalitroš, J. Pavlik, R. Boča, O. Fuhr, C. Rajadurai and M. Ruben, *CrystEngComm*, 2010, **12**, 2361; A. Abhervé, M. Clemente-León, E. Coronado, C. J. Gómez-García and M. López-Jordà, *Dalton Trans.*, 2014, **43**, 9406.

18 J. Elhaïk, C. M. Pask, C. A. Kilner and M. A. Halcrow, *Tetrahedron*, 2007, **63**, 291.

19 C. Rajadurai, O. Fuhr, R. Kruk, M. Ghafari, H. Hahn and M. Ruben, *Chem. Commun.*, 2007, 2636.

20 E. C. Constable, B. A. Hermann, C. E. Housecroft, M. Neuburger, S. Schaffner and L. J. Scherer, *New J. Chem.*, 2005, **29**, 1475.

21 M. J. J. Pereira Silva, P. Bertoncello, N. N. Daskalakis, N. Spencer, B. M. Kariuki, P. R. Unwin and Z. Pikramenou, *Supramol. Chem.*, 2007, **19**, 115.

22 E. P. L. van der Geer, G. van Koten, R. J. M. Klein Gebbink and B. Hessen, *Inorg. Chem.*, 2008, **47**, 2849.

23 Q. Wang, P. Day, J.-P. Griffiths, H. Nie and J. D. Wallis, *New J. Chem.*, 2006, **30**, 1790; C. W. Machan, M. Adelhardt, A. A. Sarjeant, C. L. Stern, J. Sutter, K. Meyer and C. A. Mirkin, *J. Am. Chem. Soc.*, 2012, **134**, 16921.

24 For other metallamacrocycles based on linked $[M(terpy)_2]^{n+}$ building blocks see: S.-S. Sun and A. J. Lees, *Inorg. Chem.*, 2001, **40**, 3154; G. R. Newkome, T. J. Cho, C. N. Moorefield, R. Cush, P. S. Russo, L. A. Godinez, M. J. Saunders and P. Mohapatra, *Chem. – Eur. J.*, 2002, **8**, 2946; E. C. Constable, C. E. Housecroft, M. Neuburger, S. Schaffner and E. J. Shardlow, *Dalton Trans.*, 2005, 234; E. C. Constable, E. L. Dunphy, C. E. Housecroft, W. Kylberg, M. Neuburger, S. Schaffner, E. R. Schofield and C. B. Smith, *Chem. – Eur. J.*, 2006, **12**, 4600; A. Schultz, X. Li, B. Barkakaty, C. N. Moorefield, C. Wesdemiotis and G. R. Newkome, *J. Am. Chem. Soc.*, 2012, **134**, 7672; A. Schultz, Y. Cao, M. Huang, S. Z. D. Cheng, X. Li, C. N. Moorefield, C. Wesdemiotis and G. R. Newkome, *Dalton Trans.*, 2012, **41**, 11573; T.-Z. Xie, K. Guo, M. Huang, X. Lu, S.-Y. Liao, R. Sarkar, C. N. Moorefield, S. Z. D. Cheng, C. Wesdemiotis and G. R. Newkome, *Chem. – Eur. J.*, 2014, **20**, 11291.

25 $[Fe_4(\mu\text{-CN})_4]^{8+}$ molecular squares exhibiting spin-crossover: M. Nihei, M. Ui, M. Yokota, L. Han, A. Maeda, H. Kishida, H. Okamoto and H. Oshio, *Angew. Chem., Int. Ed.*, 2005, **44**, 6484; T. Nishihara, M. Nihei, H. Oshio and K. Tanaka, *J. Phys.: Conf. Ser.*, 2009, **148**, 012033; M. Nihei, M. Ui and H. Oshio, *Polyhedron*, 2009, **28**, 1718; I. Boldog, F. J. Muñoz-Lara, A. B. Gaspar, M. C. Muñoz, M. Seredyuk and J. A. Real, *Inorg. Chem.*, 2009, **48**, 3710; R.-J. Wei, Q. Huo, J. Tao, R.-B. Huang and L.-S. Zheng, *Angew. Chem., Int. Ed.*, 2011, **50**, 8940; R.-J. Wei, J. Tao, R.-B. Huang and L.-S. Zheng, *Eur. J. Inorg. Chem.*, 2013, 916; O. Hietsoi, P. W. Dunk, H. D. Stout, A. Arroyave, K. Kovnir, R. E. Irons, N. Kassenova, R. Erkasov, C. Achim and M. Shatruk, *Inorg. Chem.*, 2014, **53**, 13070.

26 Tetrametallic grid complexes exhibiting spin-crossover: M. Ruben, E. Breuning, J.-M. Lehn, V. Ksenofontov, F. Renz, P. Gütlich and G. B. M. Vaughan, *Chem. – Eur. J.*, 2003, **9**, 4422; D.-Y. Wu, O. Sato, Y. Einaga and C.-Y. Duan, *Angew. Chem., Int. Ed.*, 2009, **48**, 1475; B. Schneider, S. Demeshko, S. Dechert and F. Meyer, *Angew. Chem., Int. Ed.*, 2010, **49**, 9274; A. R. Stefankiewicz, G. Rogez, J. Harrowfield, A. N. Sobolev, A. Madalan, J. Huuskonen, K. Rissanen and J.-M. Lehn, *Dalton Trans.*, 2012, **41**, 13848; Y.-T. Wang, S.-T. Li, S.-Q. Wu, A.-L. Cui, D.-Z. Shen and H.-Z. Kou, *J. Am. Chem. Soc.*, 2013, **135**, 5942; T. Matsumoto, G. N. Newton, T. Shiga, S. Hayami, Y. Matsui, H. Okamoto, R. Kumai, Y. Murakami and H. Oshio, *Nat. Commun.*, 2014, **5**, 3865.

27 Tetrahedral coordination cages exhibiting spin-crossover: A. Ferguson, M. A. Squire, D. Siretanu, D. Mitcov, C. Mathonière, R. Clérac and P. E. Kruger, *Chem. Commun.*, 2013, **49**, 1597; R. A. Bilbeisi, S. Zarra, H. L. C. Feltham, G. N. L. Jameson, J. K. Clegg, S. Brooker and J. R. Nitschke, *Chem. – Eur. J.*, 2013, **19**, 8058; D.-H. Ren, D. Qiu, C.-Y. Pang, Z. Li and Z.-G. Gu, *Chem. Commun.*, 2015, **51**, 788.

28 Other spin-crossover compounds with high nuclearity: M. Shatruk, A. Dragulescu-Andrasi, K. E. Chambers, S. A. Stoian, E. L. Bominaar, C. Achim and K. R. Dunbar, *J. Am. Chem. Soc.*, 2007, **129**, 6104; M. B. Duriska, S. M. Neville, B. Moubaraki, J. D. Cashion, G. J. Halder, K. W. Chapman, C. Balde, J.-F. Létard, K. S. Murray, C. J. Kepert and S. R. Batten, *Angew. Chem., Int. Ed.*, 2009, **48**, 2549; R. Boča, I. Šalitroš, J. Kožíšek, J. Linares, J. Moncol and F. Renz, *Dalton Trans.*, 2010, **39**, 2198; M. B. Duriska, S. M. Neville, B. Moubaraki, K. S. Murray, C. Baldé, J.-F. Létard, C. J. Kepert and S. R. Batten, *ChemPlusChem*, 2012, **77**, 616.

29 G. B. Barlin, D. J. Brown and M. D. Fenn, *Aust. J. Chem.*, 1984, **37**, 2391.

30 H.-Z. Yu, Y.-M. Yang, L. Zhang, Z.-M. Dang and G.-H. Hu, *J. Phys. Chem. A*, 2014, **118**, 606.

31 C. A. Bessel, R. F. See, D. L. Jameson, M. R. Churchill and K. J. Takeuchi, *J. Chem. Soc., Dalton Trans.*, 1992, 3223.

32 I. Bertini and C. Luchinat, *NMR of paramagnetic substances*, *Coord. Chem. Rev.*, 1996, **150**, 292.

33 S. F. Lincoln, *Helv. Chim. Acta*, 2005, **88**, 523.

34 W. J. Geary, *Coord. Chem. Rev.*, 1971, **7**, 81; R. K. Boggess and D. A. Zatko, *J. Chem. Educ.*, 1975, **52**, 649.

35 See *e.g.*: A. Davison, D. V. Howe and E. T. Shawl, *Inorg. Chem.*, 1967, **6**, 458; R. L. Dutta, D. W. Meek and D. H. Busch, *Inorg. Chem.*, 1970, **9**, 1215; S. Ruttimann, C. Piguet, G. Bernardinelli, B. Bocquet and A. F. Williams, *J. Am. Chem. Soc.*, 1992, **114**, 4230; N. C. Habermehl, P. M. Angus, N. L. Kilah, L. Norén, A. D. Rae, A. C. Willis and S. B. Wild, *Inorg. Chem.*, 2006, **45**, 1445.

36 R. D. Feltham and R. G. Hayter, *J. Chem. Soc.*, 1964, 4587.

37 P. H. Smith, Z. E. Reyes, C.-W. Lee and K. N. Raymond, *Inorg. Chem.*, 1988, **27**, 4154.

38 S. A. Willis, T. Stait-Gardner, A. S. Virk, R. Masuda, M. Zubkov, G. Zheng and W. S. Price, in *Modern NMR Techniques for Synthetic Chemists*, ed. J. Fisher, CRC Press, Baton Rouge, FL, USA, 2013, ch. 4, p. 125–176.

39 J. E. Beves, E. C. Constable, C. E. Housecroft, M. Neuburger, S. Schaffner and E. J. Shardlow, *Dalton Trans.*, 2007, 1593.

40 E. C. Constable, K. Harris, C. E. Housecroft and M. Neuburger, *Dalton Trans.*, 2011, **40**, 1524.

41 Y.-T. Chan, X. Li, J. Yu, G. A. Carri, C. N. Moorefield, G. R. Newkome and C. Wesdemiotis, *J. Am. Chem. Soc.*, 2011, **133**, 11967.

42 V. V. Krishnan, *J. Magn. Reson.*, 1997, **124**, 468.

43 M. S. Kaucher, Y.-F. Lam, S. Pieraccini, G. Gottarelli and J. T. Davis, *Chem. – Eur. J.*, 2005, **11**, 164.

44 R. Davi and D. Ben-Amotz, *Chem. Phys.*, 1994, **183**, 385.

45 J. M. Holland, J. A. McAllister, C. A. Kilner, M. Thornton-Pett, A. J. Bridgeman and M. A. Halcrow, *J. Chem. Soc., Dalton Trans.*, 2002, 548.

46 S. A. Barrett, C. A. Kilner and M. A. Halcrow, *Dalton Trans.*, 2011, **40**, 12021.

47 N. Hassan, A. B. Koudriavtsev and W. Linert, *Pure Appl. Chem.*, 2008, **80**, 1281.

48 R. Pritchard, C. A. Kilner, S. A. Barrett and M. A. Halcrow, *Inorg. Chim. Acta*, 2009, **362**, 4365; R. Mohammed,

G. Chastanet, F. Tuna, T. L. Malkin, S. A. Barrett, C. A. Kilner, J.-F. Létard and M. A. Halcrow, *Eur. J. Inorg. Chem.*, 2013, 819.

49 G. M. Sheldrick, *Acta Crystallogr., Sect. A: Fundam. Crystallogr.*, 2008, **64**, 112.

50 L. J. Barbour, *J. Supramol. Chem.*, 2001, **1**, 189.

51 *POVRAY, v. 3.5*, Persistence of Vision Raytracer Pty. Ltd, Williamstown, Victoria, Australia, 2002. http://www.povray.org.

52 C. J. O'Connor, *Prog. Inorg. Chem.*, 1982, **29**, 203.

53 D. F. Evans, *J. Chem. Soc.*, 1959, 2003; E. M. Schubert, *J. Chem. Educ.*, 1992, **69**, 62.

54 J. C. Philip and H. B. Oakley, *J. Chem. Soc., Dalton Trans.*, 1924, 1189.

55 *SIGMAPLOT, v. 8.02*, SPSS Scientific Inc., Chicago, IL, 2002.

56 M. D. Pelta, H. Barjat, G. A. Morris, A. L. Davis and S. J. Hammond, *Magn. Reson. Chem.*, 1998, **36**, 706.

57 M. D. Pelta, G. A. Morris, M. J. Stchedroff and S. J. Hammond, *Magn. Reson. Chem.*, 2002, **40**, S147.